Am J Physiol Cell Physiol 292: C1536–C1542, 2007.
First published November 22, 2006; doi:10.1152/ajpcell.00348.2006.

Production of a uniform cellular injury by raster scanning of cells for the study of laser bioeffects

K. P. Walker III,[1] S. T. Schuschereba,[1] P. R. Edsall,[1] B. E. Stuck,[1] and P. D. Bowman[2]

[1]*U.S. Army Medical Research Detachment, Brooks City-Base, Texas; and*

[2]*U.S. Army Institute of Surgical Research, Fort Sam Houston, Texas*

Submitted 30 June 2006; accepted in final form 17 November 2006

Walker KP III, Schuschereba ST, Edsall PR, Stuck BE, Bowman PD. Production of a uniform cellular injury by raster scanning of cells for the study of laser bioeffects. *Am J Physiol Cell Physiol* 292: C1536–C1542, 2007. First published November 22, 2006; doi:10.1152/ajpcell.00348.2006.—Efforts to understand laser bioeffects in cells and tissues have been hindered by a nonuniform cellular response of the specimen, resulting in graded biochemical effects. In addition, the small beam diameters of commonly used lasers limit the number of cells expressing a response to numbers inadequate for the study of biochemical effects. For a limited emission power, expansion of the beam diameter reduces the irradiance, thus requiring longer exposure durations to produce a cellular response. Cultured human retinal epithelial cells were exposed as a single spot ("tophat" exposure) from a carbon dioxide (CO_2) laser operating at 10.6 μm or scanned with a raster system and compared with thermal injury produced with heated saline for short periods (1–9 s) at relatively high temperature (55–70°C). Cell viability and induction of the 70 kDa heat shock protein were evaluated as indicators of the cellular response. Initial attempts to use a tophat (uniform energy distribution) exposure resulted in a nonuniform cellular response (and nonuniform energy distribution) due to diffraction effects from the 2-mm selection aperture. However, raster scanning for appropriate times with the CO_2 laser yielded uniform cell viability and heat shock protein synthesis that were comparable to dipping cells in heated saline. Because scanning results in a homogeneous exposure of cells, the described scanning technique may be applied to studies of cellular responses to other lasers to evaluate photochemical and photomechanical effects.

carbon dioxide laser

LASERS ARE INCREASINGLY FOUND in medical applications particularly in the area of eye surgery being used for photocoagulation and refractive surgery. Along with this increased use comes the elevated possibility of injury from their use and the need for methods to ameliorate these injuries. In the effort to understand laser-tissue interactions, a variety of animal models have been examined (12, 17, 19, 20). Much has been learned about how laser light can damage biologic tissue, especially the retina. However, most of what we know from animal models is based on morphological data (7–13). Because the injuries are small and result in poor signal-to-noise ratios of any released biochemical/molecular signals, biochemical and molecular data have not been obtained. Therefore it has been difficult to formulate therapeutic measures based on a thorough understanding of the underlying injury. The objective of this study, therefore, is to design a means of producing a uniform injury so that a homogeneous response to laser exposure could be obtained with sufficient numbers of cells to facilitate analysis at the molecular level.

Retinal pigment epithelial (RPE) cell changes are observed by histopathology after visible laser exposure at doses near the ophthalmoscopic minimal visible lesion threshold for exposure conditions where the interaction mechanism is photothermal (8). Collimated, visible laser light incident upon the cornea is transmitted through the outer ocular media and imaged or focused onto the sensory retina where it is primarily absorbed (albeit partially) by the melanin located in or near the RPE and the choroid. Absorption of the radiation by melanin in the RPE results in a localized temperature elevation with subsequent dissipation of the energy throughout the cells or surrounding tissue by thermal diffusion. If the integrated temperature-time history is sufficient (20), thermal injury to the cell and adjacent tissue is produced.

RPE cells in culture were selected to characterize the cellular response to a laser-induced insult. Since our human adult RPE (ARPE) cells contained no melanin and therefore would absorb minimally if illuminated with visible laser radiation, we chose to use a carbon dioxide (CO_2) laser to stimulate the cells, as 90% of the 10.6-μm radiation is absorbed in the first 30 μm of cells and media. Hence, exposure of a thin monolayer (10 μm) of RPE cells plus residual media (7 μm) at 10.6 μm results in absorption of 75% of the incident radiation in this small volume with a concomitant temperature elevation. An established thermal dipping technique known to produce a uniform cellular response (4) was used for comparison.

To study the bioeffects of laser exposure, techniques were explored to produce a uniform cellular response in a sufficient number of cells, so that biochemical analysis could be performed. Use of a small Gaussian beam would not result in the desired uniform cellular response; hence, a uniform intensity distribution ("tophat") was attempted. Finally, a raster scanning approach was developed which produced the desired uniform cellular response over a large number of cells.

MATERIALS AND METHODS

Cell culture. ARPE-19 cells, derived from human retinal pigment epithelium (5, 6), were a gift from Dr. Larry Hjelmeland, Department of Ophthalmology, University of California at Davis. Stock cultures were grown in T75 flasks in DMEM (GIBCO-BRL, Life Technologies, Grand Island, NY) supplemented with 10% fetal bovine serum (FetalClone III, Hyclone, Logan, UT), 100 μg/ml penicillin/streptomycin, and 5 μg/ml Fungizone (GIBCO-BRL Life Technologies) at 37°C, 5% CO_2-95% relative humidity.

Cells were seeded onto glass-bottomed 35-mm Petri dishes (MatTek Ashland, MA) or 24-well culture plates (Corning, Corning, NY). The 35-mm dishes are fitted with a 14-mm diameter opening in the

Address for reprint requests and other correspondence: P. Bowman, U.S. Army Institute of Surgical Research, 3400 Rawley E. Chamber Ave., Fort Sam Houston, TX 78234-6315 (e-mail: phillip.bowman@amedd.army.mil).

The costs of publication of this article were defrayed in part by the payment of page charges. The article must therefore be hereby marked "*advertisement*" in accordance with 18 U.S.C. Section 1734 solely to indicate this fact.

Report Documentation Page

Form Approved
OMB No. 0704-0188

1. REPORT DATE	2. REPORT TYPE	3. DATES COVERED
01 MAY 2007	**N/A**	**-**

4. TITLE AND SUBTITLE	5a. CONTRACT NUMBER
Production of a uniform cellular injury by raster scanning of cells for the study of laser bioeffects	5b. GRANT NUMBER
	5c. PROGRAM ELEMENT NUMBER
6. AUTHOR(S)	5d. PROJECT NUMBER
Walker K. P., Schuschereba S. T., Edsall P. R., Stuck B. E., Bowman P. D.,	5e. TASK NUMBER
	5f. WORK UNIT NUMBER
7. PERFORMING ORGANIZATION NAME(S) AND ADDRESS(ES)	8. PERFORMING ORGANIZATION REPORT NUMBER
United States Army Institute of Surgical Research, JBSA Fort Sam Houston, TX 78234	
9. SPONSORING/MONITORING AGENCY NAME(S) AND ADDRESS(ES)	10. SPONSOR/MONITOR'S ACRONYM(S)
	11. SPONSOR/MONITOR'S REPORT NUMBER(S)

12. DISTRIBUTION/AVAILABILITY STATEMENT
Approved for public release, distribution unlimited

13. SUPPLEMENTARY NOTES

14. ABSTRACT

15. SUBJECT TERMS

16. SECURITY CLASSIFICATION OF:			17. LIMITATION OF ABSTRACT	18. NUMBER OF PAGES	19a. NAME OF RESPONSIBLE PERSON
a. REPORT	b. ABSTRACT	c. THIS PAGE			
unclassified	**unclassified**	**unclassified**	**UU**	**7**	

center dish to which is glued a coverslip. Coverslips were precoated with Pronectin (Sanyo Chemical Industries, Kyoto, Japan) to aid in cell adhesion.

Laser experiments. A carbon dioxide laser system (model UL-30-OEM; Universal Laser Systems, Scottsdale, AZ) with a wavelength of 10.6 μm and energy output of 30 W was used for irradiating cultured cells. The beam was directed through a 2-mm aperture, and the resulting energy past the aperture, as measured by a power meter (model 210, Coherent Radiation), was 2 W. The length of time that the cells were exposed to this energy was the principal variable. The configuration of the laser equipment used for the determination of the beam profile is shown in Fig. 1*A* and that used for the single spot ("tophat") and raster scanning is shown in Fig. 1*C*, and Fig. 1*B* details the placement of the aperture at different distances from the cell layer.

Single-spot carbon dioxide laser irradiation. In an attempt to deliver a uniform ("tophat") irradiance to the cells, the center portion of the diverged beam with a uniform irradiance was directed through a 2-mm machined aluminum aperture (Fig. 1*B*). The distance from the 2-mm aperture to the cell monolayer was varied from 0.1 to 8 cm with a rack and pinion micropositioner. The total power through the 2-mm aperture was 0.9 W. The cellular response was then characterized for exposure durations from 10 to 250 ms.

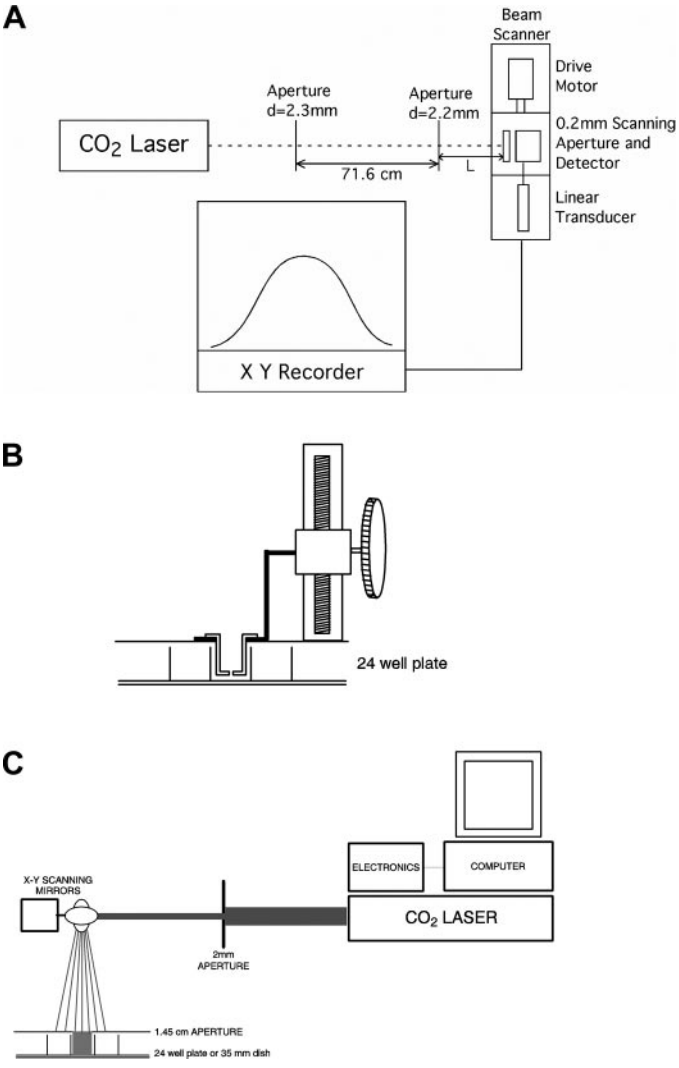

Fig. 1. *A*: schematic of laser setup for determination of beam profile. *B*: schematic of configuration of apparatus used to determine the tophat profile of the laser beam at successive distances from a 2.2-mm aperture. *C*: schematic showing setup for laser raster scanning of large numbers of cultured cells in monolayers.

Determination of energy distribution across the beam profile. A continuous wave carbon dioxide laser with a near-Gaussian exit beam diameter of 5.2 mm at the 1/e points was directed through a 2.3-mm aperture and used for determining the energy distribution across the beam profile. A second aperture of 2.2 mm located 72 cm from the first aperture was used to assess the diffraction effects from a 2.2-mm aperture (Fig. 1*A*). The intensity distribution at the second aperture was measured with an automated beam-scanning device consisting of a 50-μm thermocouple (SiO_2) located behind and thermally isolated from a 0.2-mm selection aperture. The scanning device included a linear transducer that provided an output voltage proportional to the displacement of the selection detector. As the device was moved across the beam, the outputs of the thermocouple detector (y) and transducer (x) were recorded.

Carbon dioxide laser irradiation by scanning. The laser beam was directed to a set of computer-controlled X-Y scanning mirrors, (model Z1913; General Scanning, Watertown, MA) mounted perpendicular to each other, which scanned the beam in a raster pattern across a 14.5-mm limiting aperture resulting in a circular 16-mm diameter footprint at the level of the well (Fig. 1*C*). The raster scan consisted of 100 individual lines spanning a 23 mm by 21 mm rectangular area, which overfilled the 14.5-mm aperture. Thermal response paper taped to a black steel base was exposed to the scan to generate an alignment target for the well bottoms beneath the aperture for exposure.

For irradiation, each confluent well was exposed to a single scan of the raster. Because the scan line offset of 0.2 mm is less than the 2-mm beam diameter, each cell on the advancing edge received ~10 exposures of varying thermal intensity, as the beam was rapidly and repetitively scanned across it. The irradiance of the 2-W, 2-mm diameter laser beam was 64 W/cm^2. The computer-controlled raster scan was varied in total scan time to adjust the dwell time of the laser beam on the cells. For a 10 μm^2 area, or approximately the estimated surface area of a cell, the calculated total exposure time was ~41.4 ms for a 5-s scan, and the total irradiant energy was 0.21 μJ. In the experiments described here, total scan times ranged from 5 to 15 s, corresponding to time-averaged irradiant energy doses ranging from 2.1 J/cm^2 to 6.3 J/cm^2 averaged over the whole monolayer of cells, as shown in Table 1.

Immediately before irradiation, the medium was carefully aspirated from out of the well bottom with a microtip pipette. A critical factor for exposure reproducibility required uniform removal of the medium, as water is the main absorber at 10.6 μm. Next, the well bottom was aligned with the target, and the scanning sequence was activated by computer control. Immediately after exposure, 0.5 ml of fresh medium was added into each well, and plates were returned to a 37°C incubator (95% O_2-5% CO_2/95% relative humidity). Cells were followed by microscopy and cell viability assays.

Heated saline injury experiments. Thermal injury experiments were carried out after the cells reached confluence by dipping the cultured cells on a glass-bottomed Petri dish into 0.9% saline heated to 55°C in a circulating waterbath (HAAKE D1, Berlin, Germany) for various periods of time as previously described (1). Briefly, when continuous monitoring of the circulating saline with a Physitemp BAT-10 thermometer and IT-18 microprobe (Physitemp, Clifton, NJ) indicated that the temperature of the medium had stabilized, culture dishes were immersed and then immediately dipped into room temperature saline. Each culture dish immediately thereafter received medium at room temperature and was returned to the incubator. At least three culture dishes were treated for each temperature or time point.

Cell viability. At different times after heating, cells were assayed for viability with a modification of the method described by Mosman (16). Each well received 0.5 mg/ml 3-(4,5-dimethylthiazol-2-yl) 2,5-diphenyl tetrazolium bromide (MTT, Sigma, St. Louis, MO) in PBS (pH 7.4). At the end of 15 min, the medium was removed and

Table 1. *Irradiation scan times and exposure levels*

Total Scan Time, s	Averaged Exposure, J/cm^2	Averaged Exposure, μJ/10 μm^2	Integrated Cell Exposure Time, ms
5	2.1	0.21	41.4
6	2.5	0.25	49.7
7	2.9	0.29	58.0
8	3.3	0.33	66.3
9	3.8	0.38	74.5
10	4.2	0.42	82.8
11	4.6	0.46	91.1
12	5.0	0.50	99.4
13	5.4	0.54	107.7
14	5.8	0.58	115.9
15	6.3	0.63	124.2

replaced with PBS without MTT, and cells were photographed for analysis of the distribution of the formazan.

To determine the optimal time of exposure for producing a sublethal thermal injury, preliminary experiments using increasing times of heating (0–9 s) with a constant temperature of 55°C were carried out with cells grown on Thermanox coverslips (Nalge Nunc International, Rochester, NY). The percentage of cells viable at 24 h postheating was determined for each experiment, using mitochondrial MTT redox activity as an indicator.

Heat shock protein 70 immunolocalization. For demonstration of heat shock protein (hsp70) production by heat exposure, treated or untreated cells were fixed with cold ethanol:acetone (1:1) for 5 min 6 h after saline or laser heating. They were then placed in blocking buffer (0.2% iBlock, 0.1% Tween 20, and 0.1% thimerosal in PBS; Tropix, Bedford, MA). After 10–30 min in blocking buffer, the cell layer was exposed to alkaline phosphatase-conjugated mouse monoclonal antibody against hsp70 (Stressgen, Vancouver, BC) for 1–3 h. At the end of the incubation, the cell layer was washed twice with blocking buffer, once with Tris-buffered saline pH 9.0 containing 50 mM magnesium and then incubated in 5-bromo-4-chloro-3-indolyl phosphate/nitro blue tetrazolium (BCIP/NBT Zymed/Invitrogen, Carlsbad, CA) for 5–40 min for localization of hsp70.

Western blot analysis. ARPE-19 cells were exposed in triplicate for varying times to the CO_2 laser. After 6 h, the medium was aspirated from the wells, and the cells were washed twice with PBS. Lysis of the cells was achieved by adding 200 μl of 125 mM Tris·HCl, 20% glycerol, 4% SDS, and 0.005% bromophenol blue to each well. The lysate from each well was transferred to individual 1.5 ml microcentrifuge tubes. To this was added 5 μl β-mercaptoethanol and the lysate was boiled for 3 min. Eighteen microliters per lane were loaded onto a 4–12% SDS-PAGE gel (Novex/Invitrogen, Carlsbad, CA) and electrophoresed for 35 min at a constant 200 V. The protein bands were then transferred to a nitrocellulose membrane and incubated with blocking buffer for 30 min. The membrane was then incubated with a mouse monoclonal antibody against hsp70 (Stressgen, Vancouver, BC) and simultaneously with a mouse monoclonal antibody against β-actin (Santa Cruz Biotechnology, Santa Cruz, CA) overnight. After the membrane was washed three times with PBS and Tween 20 (PBST; Sigma), the membrane was incubated with goat anti-mouse IgG antibody conjugated to alkaline phosphatase (Promega, Madison, WI) for 1.5 h. After the membrane was washed twice with PBST and once with Tris-buffered saline at pH 9.0, it was incubated with BCIP/NBT substrate until bands developed. The resulting Western blots were digitized with a flatbed scanner, and quantification was performed with Image J software (http://rsb.info.nih.gov/ij/index.html). Each experiment was performed in triplicate at least three times.

RESULTS

Figure 2 illustrates the cellular response when the cells were exposed to a CO_2 laser beam with a Gaussian irradiance distribution. The exposure duration was 150 ms, and the total incident power was 1.3 W through a 2-mm aperture located 80 cm from the cell monolayer. The 1/e beam diameter at the cell monolayer was ~4.0 mm, resulting in a peak irradiance of 10 W/cm^2. For this condition, the MTT staining showed that all cells in the center of the beam were dead, and the cells surrounding the area of lost cells (the penumbra of the lesion) were viable and exhibited enhanced MTT staining relative to the cells immediately outside this penumbra area, which appeared normal. This is possibly a hormetic effect (2, 3); that is,

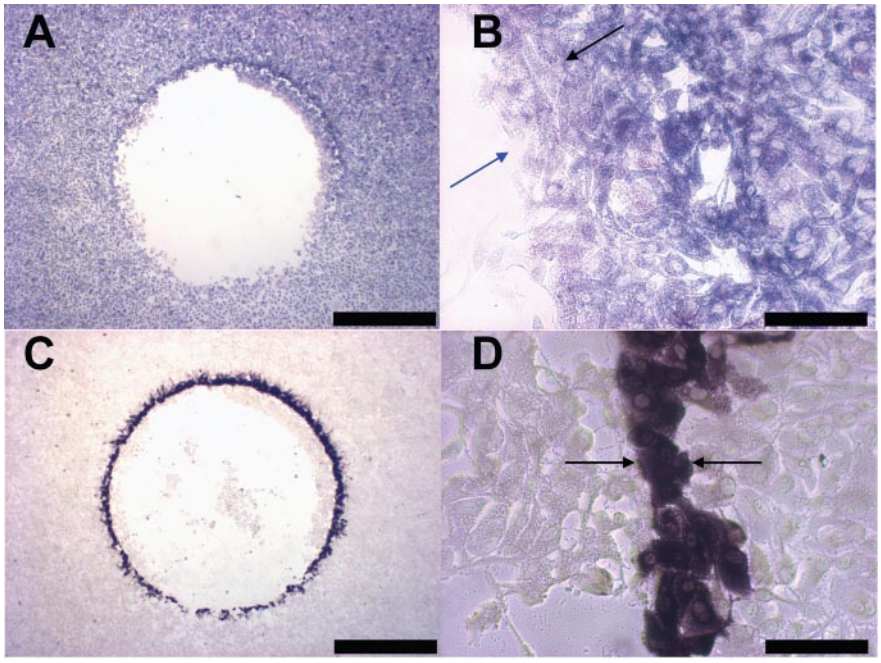

Fig. 2. 3-(4,5-dimethylthiazol-2-yl) 2,5-diphenyl tetrazolium bromide (MTT) staining of laser impact zone. Single-spot, carbon dioxide laser exposure of an adult retinal pigment epithelial (ARPE)-19 cell monolayer (10.6-μm, 4.0-mm spot size, 41.3 W/cm^2 irradiance, 150 ms duration). *A*: ×21.4 magnification showing the absence of viable cells in the center of the lesion and rounded-up cells with some formazan deposition on the edges. *B*: ×375 magnification of MTT staining showing dead cells in the center of the lesion with no formazan (blue arrow) and viable cells on the edge (black arrow). *C:* ×21.4 magnification of laser impact zone with in situ immunolocalization of hsp70 showing the thin zone of affected cells exhibiting hsp70 induction. *D*: ×375 magnification of cells about the edge of the lesion showing lack of staining in center, responders (demarcated with black arrows) grading into nonresponders outside the impact zone. Scale bars = 2 mm in *A* and *C* and 100 μm in *C* and *D*. In studies of such lesions, only a small fraction of cells are responders, resulting in poor signal-to-noise ratios for biochemical and molecular studies.

a phenomenon characterized by a low-dose stimulation, high-dose inhibition. The cells in the center of the lesion are heat-fixed and have undergone accidental cell death (14). This area grades into the remaining unirradiated cell layer with a uniform, lower level of MTT deposition. The punctate pattern of formazan distribution represents the reduction of formazan within mitochondria.

Figure 2*C* illustrates the typical intense hsp70 staining provided by the alkaline phosphatase product of BCIP/NBT that is only observed on the edges of the beam impact zone in viable cells. At higher magnification (Fig. 2*D*), a zone of 2 or 3 cells in width shows a good heat shock response. This small area grades into the unirradiated cells that exhibit no hsp70 staining.

The cells at the edge of the injury zone are the only ones available for analysis of the response to the irradiation. This result was observed repeatedly with all exposures over 100 ms. Reducing the time of exposure results in only a very small number of cells being affected in the center of the irradiation zone.

To better understand the distribution of energy across the beam profile and to develop conditions to improve tophat irradiation, a study was undertaken using the setup in Fig. 1*B* to see whether varying the distance of the aperture from the cell layer could improve the energy distribution.

As a function of distance, the beam profile results in patterns of energy distribution that are even more nonuniform. The intensity distribution through the center of the beam at the location of the 2.2-mm aperture was approximately uniform. This allowed assessment of the diffraction effects of a plane wave incident on a 2.2-mm aperture as a function of distance from the aperture. A series of profiles through the center of the beam were performed in 1-cm increments from the 2.2-mm aperture out to 20 cm. The peak irradiance just beyond the aperture was 0.4 (arbitrary units) and increased to 1.0 at a distance of 10.1 cm from the 2.2-mm aperture, and all intensity distributions were normalized to this peak. This peak intensity was ~2.5 times the peak intensity incident on the 2.2-mm aperture. In the near field (Fresnel zone) of the diffraction pattern ($L < 10$ cm) the intensity distribution varies from a series of rings to an effective focusing effect at 11 cm (data not shown). As the distance from the aperture increases to ~30 cm,

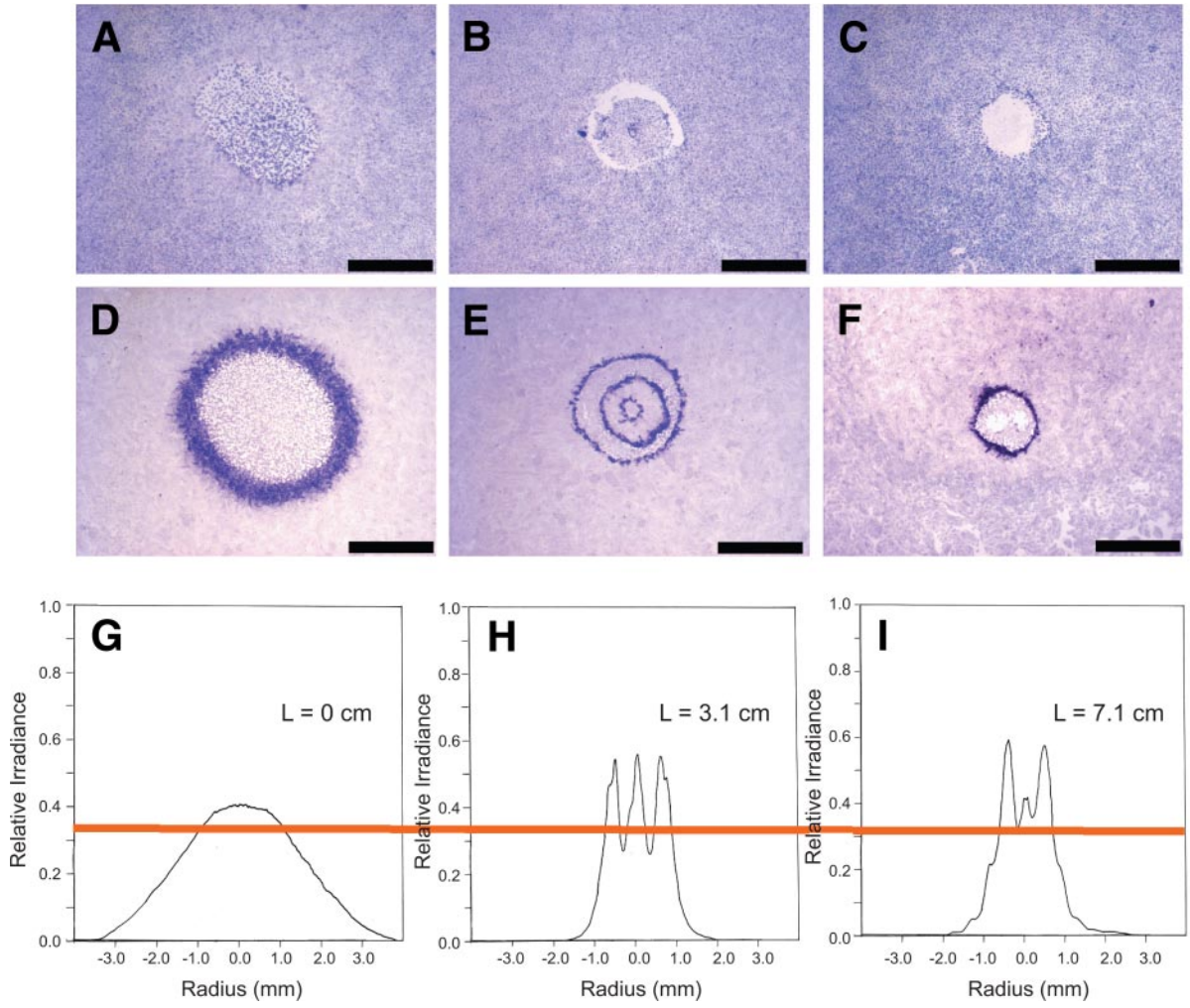

Fig. 3. Effect of CO_2 laser exposure on ARPE-19 cell monolayer. *A*, *D*, and *G*: effect of a 22.5-ms exposure from the 6-mm CO_2 laser beam on ARPE-19 cells at ×20 magnification as assayed by MTT staining (*A*) or hsp70 immunolocalization (*D*) with the energy profile of the beam (*G*). *B*, *E*, and *H*: effect of the same exposure when the beam is directed through a 2-mm aperture 3.1 cm above the cell monolayer. *C*, *F*, and *I*: effect of the same exposure with the aperture at 7.1 cm above the cell monolayer. The orange bar was arbitrarily placed to visualize the threshold (unquantified) for hsp70 induction from thermal injury as observed in *D*, *E*, and *F*. Scale bars = 2 mm.

the beam profile returns to a near-Gaussian distribution with a peak irradiance about two-thirds of that at the 2.2-mm aperture.

Figure 3 shows that the variation due to diffraction and interference as light passes through an aperture designed to obtain a tophat exposure is also reflected in the response of a cell layer.

The cells used in this study are sensitive to thermal injury, and there is apparently a threshold for the induction of hsp70 that exists as a narrow band (Fig. 3, *G–I*). As the energy profile of the beam crosses that band, hsp70 expression is induced. If the beam profile is above the band, the cells die, and if it dips below the band, the cells are alive yet not induced to produce hsp70. In the no aperture exposure (Fig. 3, *A* and *D*), the band of cells induced to produce hsp70 is relatively wide due to the gentle slope of the beam profile allowing more cells to be within the threshold band. The cells in the center are dead because the peak of the Gaussian is above the threshold. Three concentric circles are apparent in the 3.1-cm exposure (Fig. 3, *B* and *E*) with live and dead cells occurring where the beam profile dips below or rises above the threshold band. In the 7.1-cm exposure (Fig. 3, *C* and *F*), a ring of hsp70-positive cells exists around an area of dead cells. While the beam profile has peaks and valleys, the minima for the valleys are still above the threshold for hsp70 induction, and therefore all of the cells die. The beam profile is also narrower at the level of the threshold, making the resulting exposure ring of a smaller diameter than that of the 3.1-cm exposure.

Figure 4 illustrates that raster scanning as described in Fig. 1*C* produces a uniform hsp70 immunocytochemical staining pattern very similar to the one produced by dipping in saline at 55°C for 2 s. The images are representative of three separate experiments, each of which was carried out in triplicate. Figure 4, *A–C*, shows untreated controls at low- and medium-power magnification with little staining for hsp70. Figure 4, *D–F*, shows the pattern of hsp70 found after a 2-s exposure to 55°C saline followed by a 6-h delay before fixation and staining. This produces a strong, uniform staining over the cell layer. The differences in intensity of hsp70 staining between cells probably indicate that not all cells respond the same to this treatment.

Figure 4, *G–I*, shows that the raster scanning for 8 s produced a uniform staining across the layer similar to that produced by dipping into the heated medium. The results indicate that comparable amounts of energy were delivered to the cell layer by the dipping and scanning procedures. To estimate the amount of energy required to produce an hsp70

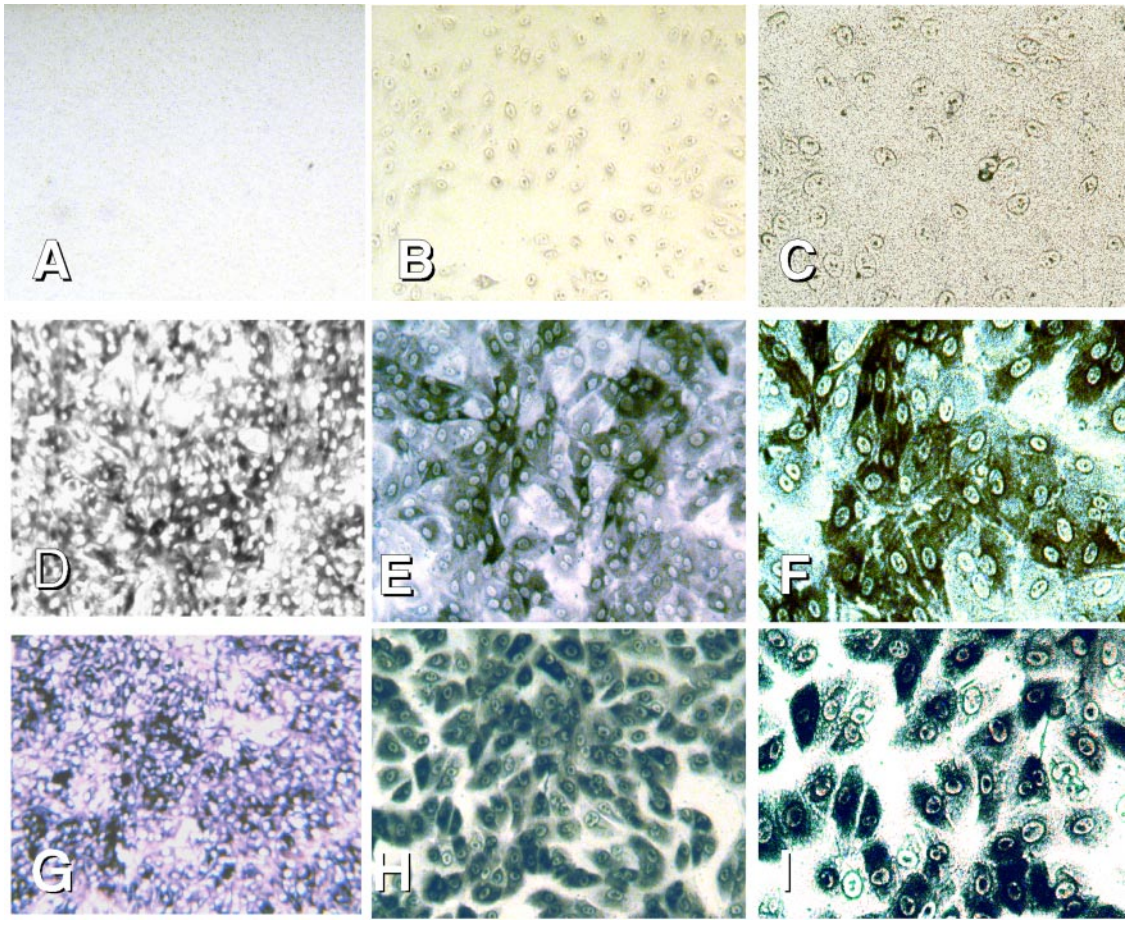

Fig. 4. Hsp70 immunostaining of control, laser, and thermally injured ARPE-19 cells. The blue-black staining denotes the presence of large amounts of hsp70 in cells. *A–C*: control cells. *D–F*: cells dipped in 55°C saline for 2 s, incubated for 6 h, and then stained for hsp70. *G–I*: cells scanned at 8 s with 2 W CO_2 laser beam. The hsp70 response between dipping and laser exposure is comparable, supporting a similar thermal mechanism. Also, large areas of the monolayer are available for further biochemical and molecular analysis, such as gel electrophoresis and gene expression analysis. Such approaches are not easily possible from animal studies. *A*, *D*, and *G*: ×12.5 magnification, *B*, *E*, and *H*: ×100 magnification, *C*, *F*, *I*: ×200 magnification.

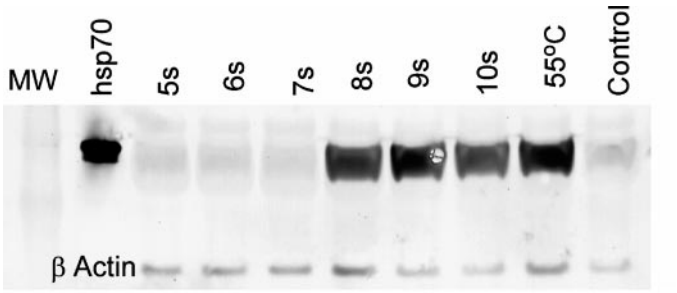

Fig. 5. Western blot analyses of cell lysates taken 6 h after exposure. A threshold of exposure by scanning was required before induction of hsp70 occurred. At 8 s, about as much hsp70 was produced as by heating for 2 s at 55°C.

response by raster scanning, Table 1 presents the relationship between scan time and energy delivery to the cell layer. On the basis of the approximate equivalence of the hsp70 staining pattern between a 2-s, 55°C exposure to heated saline and an 8-s scan time, it appears that raster scanning delivered a dose of heat equivalent to 2 s at 55°C.

Figure 5 shows Western blot analyses of representative samples exposed for varying times with the concomitant induction of the hsp70 protein. The amount of hsp70 produced is relatively constant until the cells have been heated to a threshold temperature whence production of the protein is induced and the level increases. The threshold appears to be a relatively narrow band and exposure to the laser for longer times heats the monolayer sufficiently to cause the death of cells. The exposures were made in triplicate, and the amount of hsp70 protein detected relative to β-actin is shown in Fig. 6.

Figure 7, *A* and *B*, demonstrates that the scanning procedure can be quite selective in delivery of energy. The scanning system was set to spell "USA" in the cell layer. After fixation of the cells and blocking, antibody against hsp70 was applied to the cell layer and developed as described previously. Figure 7*A* shows the cell layer at low magnification, and Fig. 7*B* shows the letter "A" at about ×80 magnification. The variability in the response of individual cells in this application may reflect variability in the responding cells or slight local variation in the film of water over the cells resulting in slight differences in the level of heating. When used in raster scanning mode, the raster overlap ensures a homogeneous response.

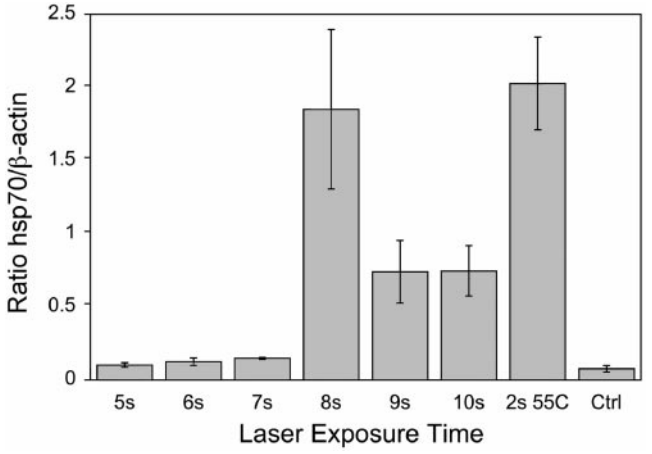

Fig. 6. Histogram comparison of averaged hsp70/β-actin ratio between scanned, heated, and untreated control cultures of ARPE19 cells. Error bars represent the SE of three replicates. At scan times beyond which a threshold for induction of hsp70 is reached, a decrease is apparent in both hsp70 and β-actin likely due to death of a portion of the population.

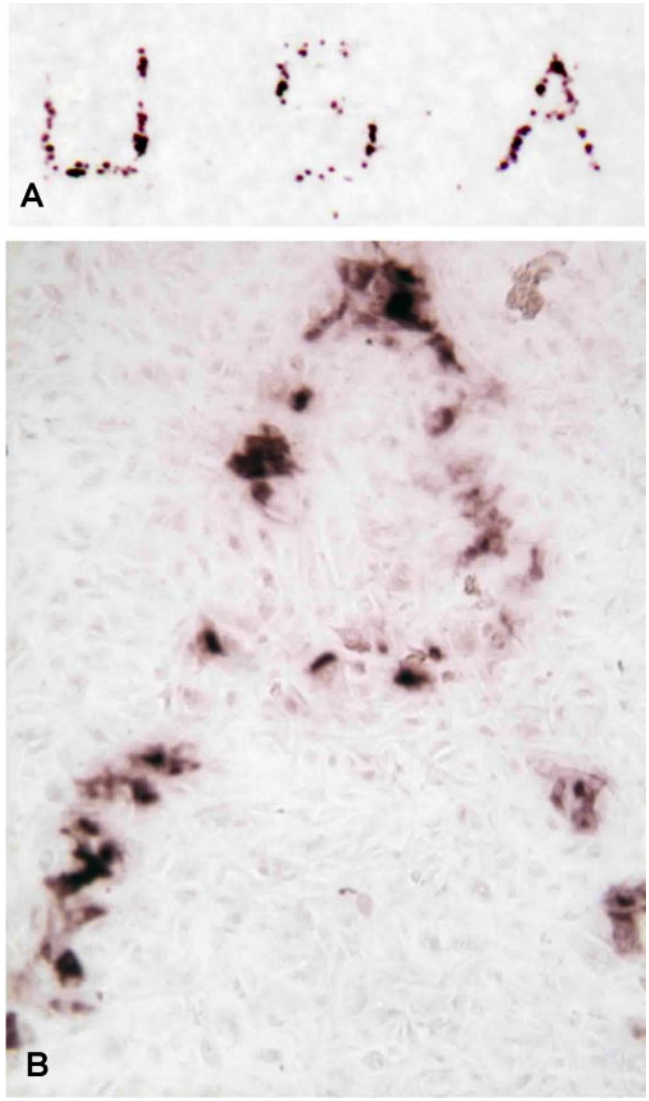

Fig. 7. The generation of "USA" in a cell layer of ARPE19 cells by sublethal heating. The scanning system was set to spell "USA" in the cell layer. After fixation of the cells and blocking, an antibody to hsp70 was applied to the cell layer and developed, as described in MATERIALS AND METHODS. The variability in the response of individual cells to the laser may reflect variability in the responding cells or slight local variation in the film of water over the cells resulting in slight differences in the level of heating.

DISCUSSION

The formulation of therapeutic means of treatment for injuries resulting from exposure to laser radiation requires knowledge of the bioeffects of such exposures. A nonuniform cellular response has hindered efforts to understand laser bioeffects in cells and tissues due to graded biochemical effects that result from the Gaussian energy distribution or diffraction and interference effects that occur when a uniform energy distribution is attempted by passing the beam through an aperture. Limited numbers of cells expressing a response from the small beam diameters of commonly used lasers have also made biochem-

ical and molecular analysis difficult to achieve. These problems have been minimized by using a computer-controlled raster scanning system that quickly sweeps across the cell layer delivering a relatively uniform amount of energy to each cell.

Depending on the length of time of the scan, from no effect to complete cell killing could be obtained. At an appropriate length of time of the scan, a uniform reduction in viability could be obtained, as indicated by a reduction of intensity of formazan staining and a uniform increase in intensity of staining for hsp70 observed in the cell layer of ARPE-19 cells. This result was comparable to the distributions seen after cells were dipped in heated media, thus suggesting that thermal effects were the predominant injury mechanisms as expected for the carbon dioxide laser. The Western blot analysis is also indicative of the fact that increasing the scan time past the threshold for hsp70 induction results in more cells killed in that the amount of hsp70 drops after 8-s exposure. That this injury is predominantly thermal was also demonstrated in early work with the carbon dioxide laser (10.6 μm) (18). This result also corresponds well to the estimation by Moritz and Henriques (15) that the basal layer of the human epidermis was killed by exposure to 65°C for 1 s.

Sufficient numbers of cells are affected by this raster scanning procedure in an area of about 1 cm^2 (about 50,000 cells) so that biochemical and molecular studies of the response and means to ameliorate it are now possible. By using different cell types and varying the scan times and irradiance levels, differential analyses may now be possible to assess laser bioeffects from a variety of laser systems and injury mechanisms.

The application of the scanning technique that we have applied to heating lasers can now be applied to laser systems that produce photochemical and photomechanical injury. In addition, the described technique may also be applied to in vivo studies.

DISCLOSURES

The opinions or assertions contained herein are the private views of the authors and are not to be construed as official or as reflecting the views of the Department of the Army or the Department of Defense.

REFERENCES

1. **Bowman PD, Schuschereba ST, Lawlor DF, Gilligan GR, Mata JR, DeBaere DR.** Survival of human epidermal keratinocytes after short-duration high temperature: synthesis of HSP70 and IL-8. *Am J Physiol Cell Physiol* 272: C1988–C1994, 1997.
2. **Calabrese EJ.** Hormesis: a revolution in toxicology, risk assessment and medicine. *EMBO Rep* 5 S37–S40, 2004.
3. **Calabrese EJ.** Toxicological awakenings: the rebirth of hormesis as a central pillar of toxicology. *Toxicol Appl Pharmacol* 204: 1–8, 2005.
4. **Dinh HK, Zhao B, Schuschereba ST, Merrill G, Bowman PD.** Gene expression profiling of the response to thermal injury in human cells. *Physiol Genomics* 7: 3–13, 2001.
5. **Dunn KC, Aotaki-Keen AE, Putkey FR, Hjelmeland LM.** ARPE-19, a human retinal pigment epithelial cell line with differentiated properties. *Exp Eye Res* 62: 155–169, 1996.
6. **Dunn KC, Marmorstein AD, Bonilha VL, Rodriguez-Boulan E, Giordano F, Hjelmeland LM.** Use of the ARPE-19 cell line as a model of RPE polarity: basolateral secretion of FGF5. *Invest Ophthalmol Vis Sci* 39: 2744–2749, 1998.
7. **Mainster MA, Crossman JL, Erickson PJ, Heacock GL.** Retinal laser lenses: magnification, spot size, and field of view. *Br J Ophthalmol* 74: 177–179, 1990.
8. **Mainster MA, White TJ, Allen RG.** Spectral dependence of retinal damage produced by intense light sources. *J Opt Soc Am A* 60: 848–855, 1970.
9. **Mainster MA, White TJ, Tips JH, Wilson PW.** Retinal-temperature increases produced by intense light sources. *J Opt Soc Am A* 60: 264–270, 1970.
10. **Marshall J, Mellerio HJ.** Histology of retinal lesions produced with Q-switched lasers. *Exp Eye Res* 7: 225–230, 1968.
11. **Marshall J, Mellerio J.** Histology of the formation of retinal laser lesions. *Exp Eye Res* 6: 4–9, 1967.
12. **Marshall J, Mellerio J.** Laser irradiation of retinal tissue. *Br Med Bull* 26: 156–160, 1970.
13. **Marshall J, Mellerio J.** Pathological development of retinal laser photocoagulations. *Exp Eye Res* 6: 303–308, 1967.
14. **Matylevitch NP, Schuschereba ST, Mata JR, Gilligan GR, Lawlor DF, Goodwin CW, Bowman PD.** Apoptosis and accidental cell death in cultured human keratinocytes after thermal injury. *Am J Pathol* 153: 567–577, 1998.
15. **Moritz AR, Henriques FCJ.** Studies of thermal injury II. The relative importance of time and surface temperature in the causation of cutaneous burns. *Am J Pathol* 23: 695–720, 1947.
16. **Mosman T.** Rapid colorimetric assay for cellular growth and survival: Application to proliferation and cytotoxicity assays. *J Immunol Methods* 65: 55–63, 1983.
17. **Schirmer KE.** Simultaneous thermal and optical breakdown mode dual laser action. *Ophthalmologica* 205: 169–177, 1992.
18. **Schuschereba ST, Ferrando RE, Stuck BE, Quong JA, Lund DJ, Bowman PD.** Stimulation of heat shock protein 70 synthesis in human fibroblasts by short duration (1 sec) carbon dioxide laser radiation. *Lasers Life Sci* 6: 27–38, 1994.
19. **Sliney DH.** Laser-tissue interactions. *Clin Chest Med* 6: 203–208, 1985.
20. **Welch AJ.** The thermal response of laser irradiated tissue. *IEEE J Quantum Electron* QE-20: 1471–1481, 1984.